5th International Conference on Water Resources and Arid Environments (ICWRAE 5): 68-76
7-9 January 2013, Riyadh, Saudi Arabia

Cloud Detection and Cloud Probability Distribution Maps Over Southern KSA Using Remote Sensing Techniques

Jarbou A. Bahrawi and Mohamed Elhag

Department of Hydrology and Water Resources Management, Faculty of Meteorology, Environment and Arid Land Agriculture, King Abdulaziz University

Abstract: Remote sensing technology have demonstrated robust capabilities in meeting challenges of water resource management, in the countries like kingdom of Saudi Arabia where rapid population growth is imposing stress on scarce water resources. Also, continuous Earth observations from space are crucial to manage water resources for the benefit of the mankind and environment, as well as to provide important forecasting services to prevent water-related disasters such as floods and droughts. Remote sensing approaches to assess and manage of water resources are important especially in the region of Saudi Arabian because no adequate hydrological networks exist. Accurate cloud detection and investigation is very important issue in extracting information of geophysical, geomorphological and meteorological interest from remotely sensed images. Present work aimed at implementing a new methodology for cloud detecting and producing cloud probability mapping of multispectral images acquired with the Medium Resolution Imaging Spectrometer (MERIS) of European Space Agency (ESA). The algorithm was implemented on 59 satellite imageries of MERIS imageries collected from January 2006 to October 2011 on monthly basis. The algorithm was performed using 9 spectral bands of MERIS imageries culminated in producing cloud probability maps and then classified into 0 and 1 maps, where 1 refereeing to cloudy pixels. The implementation of the algorithm resulted in a robust cloud probability maps over the designated area.

Key words: Classification · Cloud Detection · Cloud Probability · MERIS · Remote Sensing · Water Resources Management

INTRODUCTION

The water cycle is all about storing water and moving water on, in and above the Earth. Although the atmosphere may not be a great storehouse of water, it is the superhighway used to move water around the globe. There is always water in the atmosphere. Clouds are, of course, the most visible manifestation of atmospheric water, but even clear air contains water in particles that are too small to be seen. One estimate of the volume of water in the atmosphere at any one time is about 12,900 km^3. That may sound like a lot, but it is only about 0.001 percent of the total Earth's water volume.

Clouds exert a dominant influence on the amount of solar energy absorbed by the Earth and on the amount of infrared radiation emitted to space. It is known that clouds present a paradox they act to cool the planet by reflecting solar radiation to space and warm the planet by reducing the amount of radiation emitted to space [1, 2]. Accurate and automatic detection of clouds from remote sensing images is a key issue for a wide range of remote sensing applications, especially in the case of sensors working in the visible and near-infrared (VNIR) range of the electromagnetic spectrum [3].

Cloud screening involves discriminating between clear and cloudy pixels in an image. Cloud detection methods can be reviewed in several references, [4, 5, 6]. Methods for identifying clouds are generally based on radiance threshold, radiative transfer model, or statistical techniques making use of spectral and textural features in the imagery. Radiance threshold techniques work on a pixel-by-pixel basis and single or multiple-channel thresholds are to be defined and then can be used to divide clear and cloudy pixels. Radiative transfer model techniques use one or more spectral radiance measurements as input to an atmospheric radiative

Corresponding Auhtor: Mohamed Elhag, Department of Hydrology and Water Resources Management, Faculty of Meteorology, Environment and Arid Land Agriculture, King Abdulaziz University. E-mail: meihag@stu.kau.edu.sa.

transfer model and retrieve a physical quantity such as cloud optical thickness or altitude. The pixels are then determined to be clear or cloudy based on thresholds in the retrieved quantity. Statistical techniques use groups of adjacent pixels. Among these are methods based on spatial coherence between adjacent pixels [7] artificial neural networks [8], maximum likelihood decision rules [9] and clustering routines [10]. Specific cloud detection algorithms applied to satellite data generally have features which are beneficial for a particular scene class.

In particular, performance of the presented approach is tested on images from recent multispectral instrument with the following characteristics: the Medium Resolution Imaging Spectrometer (MERIS) instrument on board the European Space Agency (ESA) ENVISAT environmental satellite. Two of the key features of the MERIS instrument are its temporal resolution (revisit time of 3 days) and its spatial coverage (swath width of 1150 km), which make inevitable presence of cloud covers. In Reduced Resolution (RR) mode, MERIS provides 1000 m pixel-size images with 15 narrow bands fallen in the spectral range from 400 nm to 1000 nm, at unprecedented spectral and radiometric resolutions [11]. For further details see [12].

The aim of the current study is to investigate the spatiotemporal distribution of the conducted cloud probability maps over the southern part of KSA using MERIS data collected from January 2006 till October 2011.

MATERIALS AND METHODS

Study Area: Asir region is located at the southwestern part of Saudi Arabia (Figure 1). Asir covers about 100,000 km^2 of the Red Sea coastal plains, high mountains and the upper valleys of the wadis (seasonal watercourses) are Bîshah and Tathlîth. Asir is a prosperous agricultural region. It has an area of 77,088 km^2 and an estimated population of 1,563,000. It shares a short border with Yemen. Its capital is Abha. The average annual rainfall in the highlands probably ranges from 300 to 500 mm falling in two rainy seasons, the main one being in March and April with some rain in the summer. Temperatures are very extreme, with diurnal temperature ranges in the highlands the greatest in the world. It is common for afternoon temperatures to be over 30°C, yet mornings can be extremely frosty and fog can cut visibility to near zero percent. As a result, there is much more natural vegetation in Asir than in any other part of Saudi Arabia.

Cloud Probability

Algorithm Specification: The cloud probability algorithm has been developed and implemented by Free University Berlin and Brockmann Consult. It is also used in the Global MERIS Land Albedo map project [11]. The cloud probability algorithm is using nine spectral bands of MERIS. Specifically, the ratio of

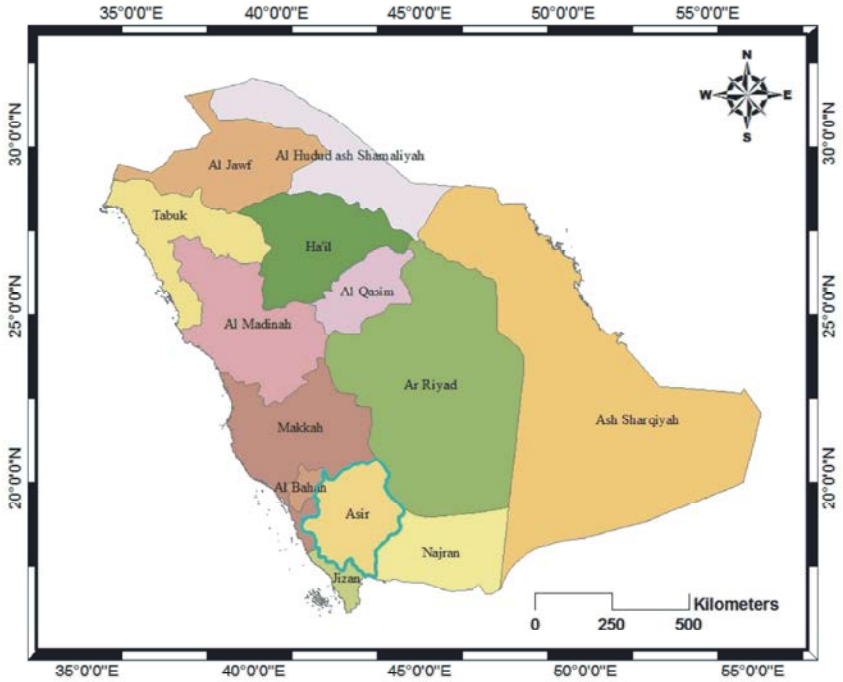

Fig. 1: Administrative boundaries of KSA regions with location of the study area highlighted

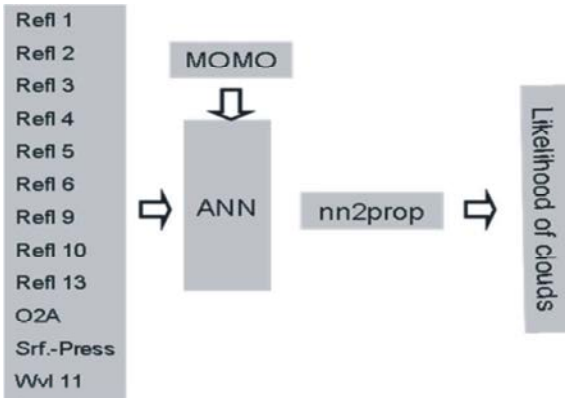

Fig. 2: Cloud detection algorithm.

band 10 (cloud optical thickness, cloud-top pressure reference), band 11 (Cloud-top / Surface pressure) and band 12 (aerosol, vegetation) which is an oxygen absorption indicator, the European Centre for Medium-Range Weather Forecasts (ECMWF) surface pressure and the exact wavelength of band 11 as input. As an output, it yields a probability value (0 to1) indicating if a pixel can be regarded as a cloud or not. Such a probability permits a more flexible way to work with identified clouds compared to a binary cloud mask.

The algorithm uses two different artificial neural networks. The first is used over the open ocean and the second over land. The distinction between ocean and land is done using the altitude information. If the altitude is lower than 50 meters then, the ocean Artificial Neural Network is not used and the land Artificial Neural Network is implemented like the current study.

Figure 2 shows the general structure of the cloud detection algorithm. During development of the algorithm by Fischer and Grassl [13]; Fell and Fischer [14], using the radiative transfer model MOMO (Matrix Operator MethOd), simulated cloud and non-cloud top of atmosphere radiance have been produced and an Artificial Neural Network has been trained. Thus, Artificial Neural Network is now used in the Cloud Probability Processor, where it is fed with the reflectance and the pressure as shown in the Figure 2. A post-processing is applied after the net (nn2prop) which scales the output of the Artificial Neural Network into a probability value.

Algorithm Basics: According to Lindstrot *et al*. [15], clouds are easily to detect when a manual classification of satellite images is done, their automatic detection is difficult. Clouds have four special radiative properties that enable their detection: 1) clouds are white, 2) clouds are bright, 3) clouds are higher than the surface and 4) clouds are cold. However clouds, as the most variable atmospheric constituent, seldom show all four properties at the same time.

Thin clouds show a portion of the underlying surface spectral properties and low clouds are sometimes quite warm. Additionally some surface types, like snow and ice have spectral properties that are very similar to some of the cloud properties. Therefore simple thresholding algorithms often fail and existing cloud detection schemes use a number of different cascaded threshold based tests to account for the complexity [16, 17].

Algorithm Specification: In general, cloud detection algorithms can be separated into two classes: clear sky conservative and cloud conservative. Clear sky conservative algorithms are constructed such that the probability of a first order error in clear sky detection is very low; in other words: if a pixel is detected as clear the probability of cloudiness should be very low. This often has the side effect that many cloud free pixels are detected as cloudy. The opposite is true for cloud conservative algorithms. Here the probability of a first order error in cloud detection is low, with the side effect that many cloudy pixels are missed.

Pure "clear sky" conservative algorithms mark pixels as cloud free or as probably cloudy, whereas pure cloud conservative algorithms detect cloudy or probably cloud free pixel. However, in practice most cloud detection algorithms try to minimize the probability of the first and second order errors in cloud and cloud free detection, only with the tendency to cloud or to clear sky conservative respectively. What kind of cloud detection algorithm should be used is mainly a question of the successive algorithm. Algorithms relying on cloudy pixels need a cloud conservative detection and vice versa; climatological applications often require balanced detection to be bias free.

MERIS measures radiances in 15 channels between 400nm and 1000nm. Thus the very valuable thermal information and information about the liquid and ice water absorption at 1.6μm and 3μm are not available. The cloud detection using MERIS, therefore, relies on bands 10, 11 and 12 according to Lindstrot *et al*. [15]. In addition a slight absorption of snow at 900nm could be used to discriminate snow from low clouds [11].

To perform the algorithm, the simulated MERIS bands radiance used to train the Artificial Neural Network to discriminate between the cloudy and cloud free. MOMO training datasets simulation used to conduct one of the three general atmospheric cases namely; a tropical,

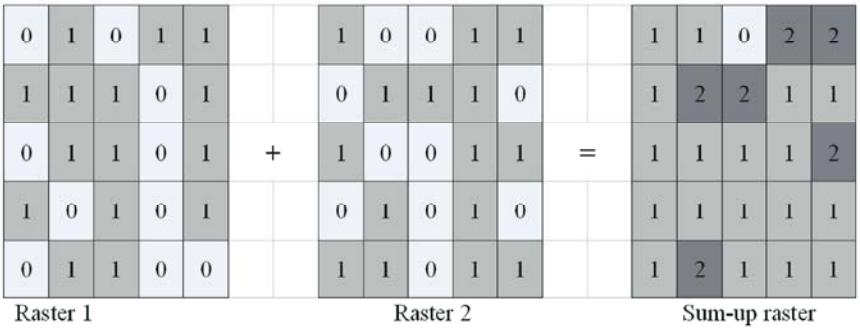

Fig. 3: Sum command illustration

Table 1: Flags used to verify the cloud probability maps of MERIS imagery

Name	Value	Description
Cosmetic	1	Pixel is cosmetic
Duplicated	2	Pixel has been duplicated (filled in)
Glint_Risk	4	Pixel has glint risk
Suspect	8	Pixel is suspect
LAND and/or OCEAN	16	Pixel is over land, not ocean
Bright	32	Pixel is bright
Coastline	64	Pixel is part of a coastline
Invalid	128	Pixel is invalid

a subarctic summer and winter and U.S. Standard Atmosphere [18]. For proper Artificial Neural Network implementation, the following inputs are required [15]:

- The radiance in MERIS band 10,
- The radiance ratio r of MERIS band 11 (stray light corrected) and the window radiance interpolated from bands 10 and 12.
- The aerosol optical thickness at 550nm (fixed to 0.15)
- The cosine of the solar incident angle
- The cosine of the viewing angle
- The cosine of the azimuth distance (viewing azimuth - solar azimuth, 0° = sensor opposite of sun) times the sinus of the viewing angle.
- The central wavelength of MERIS band 11.

To verify the certainty of the produced cloud probability maps, seven flags were used to classify the MERIS imagery data according to Table 1.

The previously mentioned procedures were followed for all MERIS data sets (59 acquired MERIS images) in order to conduct the spatiotemporal final map over the designated area.

Cell Statistics: Under ArcMap environments [19], cell statistics calculates a per-cell statistic from multiple rasters (59 raster), in the current case the "Sum" command which calculates the sum or the total of all input raster values as it is illustrated in Figure 3, is the used one for cell statistics. All raster inputs are integer; the final output is then integer and had been converted into percentages raster based on 0 and 1 cloud probability.

The final raster cloud probability map values range from 0 to 59 as the maximum total, 0 sum corresponded to 0% clouds and 59 corresponded to 100% clouds. The classification of the final spatiotemporal cloud probability map was based on Jenks rule of classification, where the output classes were based on natural groupings inherent in the data [19]. Jenks rule identifies break points by picking the class breaks that best group similar values and maximize the differences between classes. The features were divided into classes whose boundaries were set where there were relatively big jumps in the data values. The final output map were divided into three classes,

a- Not cloudy
b- Marginally cloudy and
c- Cloudy.

RESULTS AND DISCUSSION

The implementation of the algorithm over the southern part of Kingdom of Saudi Arabia (Asir region) demonstrated highly accurate results that performed under the tropical atmosphere case of Artificial Neural Network implementation [20, 15]. In a more limited study of a similar approach from March (2000), Hawkinson *et al*. [21] reported that the method determined the correct sky conditions is successful by 75% of the time. Cloud probability algorithm produced cloud maps with three levels of certainty (Figure 4): A- more than 80% of cloud probability (cloudy), B- from 80 to 20% cloud probability (marginally cloudy) and C- less than 20% cloud probability (not cloudy).

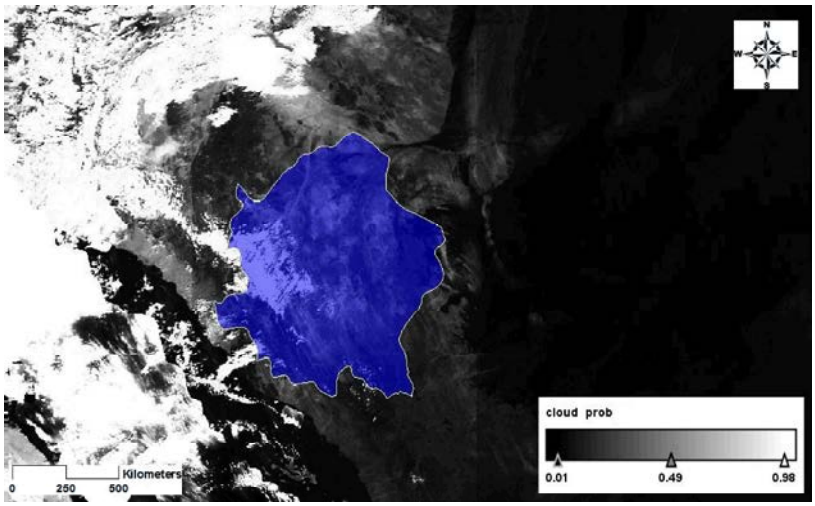

Fig. 4: Cloud certainty map over the southern part of KSA

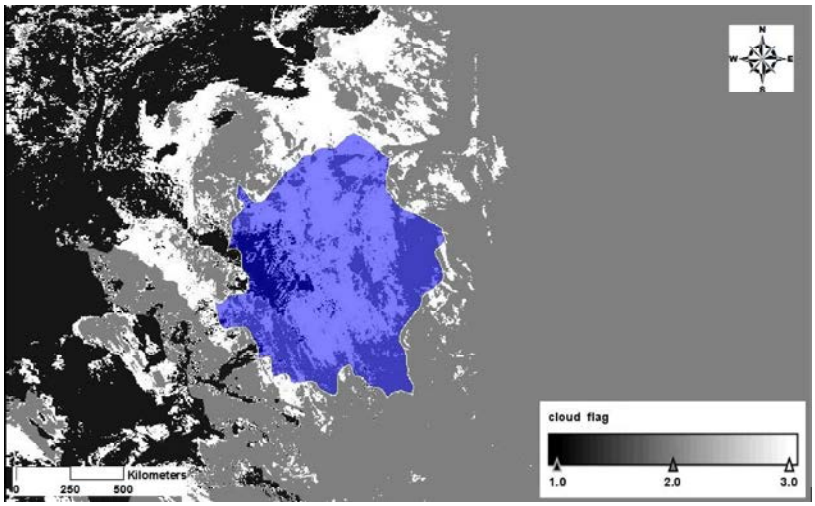

Fig. 5: Cloud probability map over the southern part of KSA

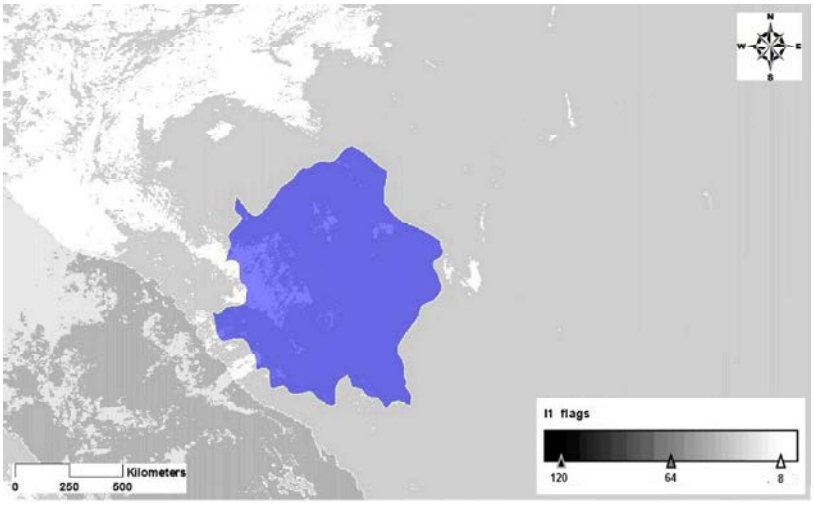

Fig. 6: Cloud probability classification flags used over the southern part of KSA

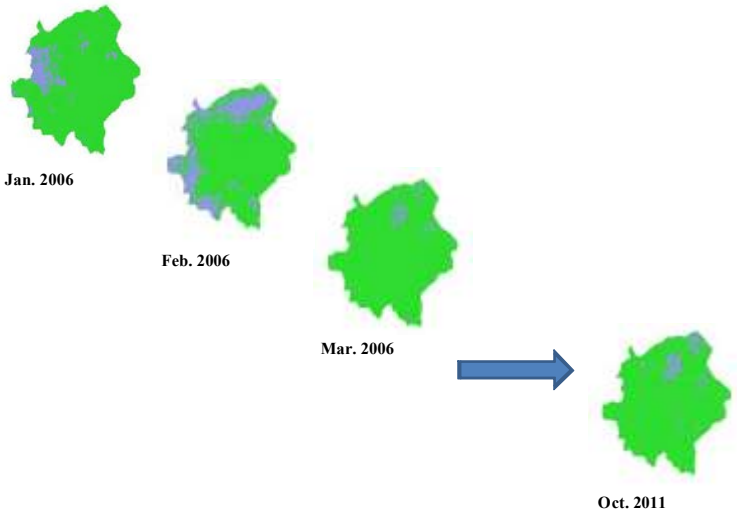

Fig. 7: Cloud probability map of 59 MERIS data set of Asir region in KSA from January 2006 to October 2011

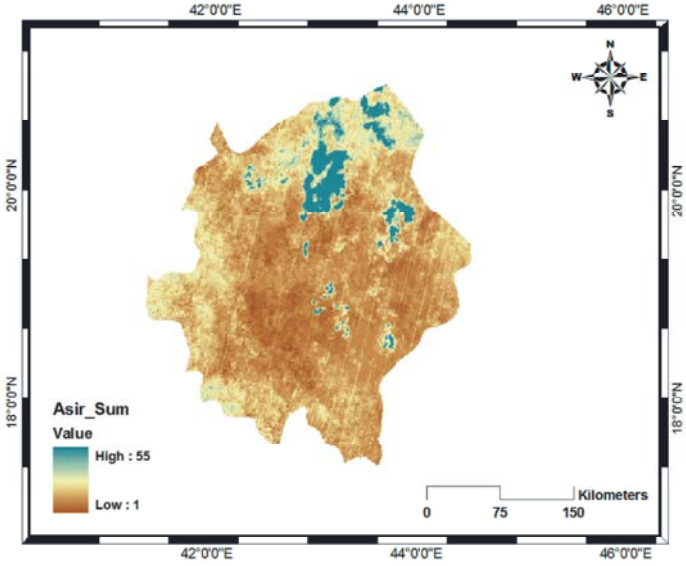

Fig. 8: Total cloud probability map of Asir region in KSA from January 2006 to October 2011

Certainty levels were converted into three cloud probability classes as shown in Figure 5. Most of the used flags belong to suspect pixels (value of 8) and to over land pixels (value of 16; Figure 6) that is to confirm the ability of the algorithm performance over the designated study area which is mainly an agricultural land and desert [22, 23, 24]. There is a significant difference between cloud free water and cloudy water pixels from Figure 6. Therefore, the clear pixels could be separated from cloudy pixels if a proper threshold value was selected. However, this is also indicated that the discrimination between land and sea by using the image of brightness temperature is successful [25].

The algorithm had been applied repeatedly to the 59 data sets of MERIS data collected and processed from January 2006 till October 2011 (Figure 7) to fulfill the defined purpose of producing spatiotemporal cloud distribution map (Figure 8). Maps with more than 80% cloud certainty were only selected to be further processed under ArcMap environment to avoid the validation of the used technique [26, 27].

Figure 9 illustrates that the spatiotemporal distribution of the clouds over Asir region for the last 5 years categorized into three category according to Jenks rule as following: not cloudy area is about: 22802 km^2 (29.5%), marginally cloudy area is about: 53141km^2 (69.0%)

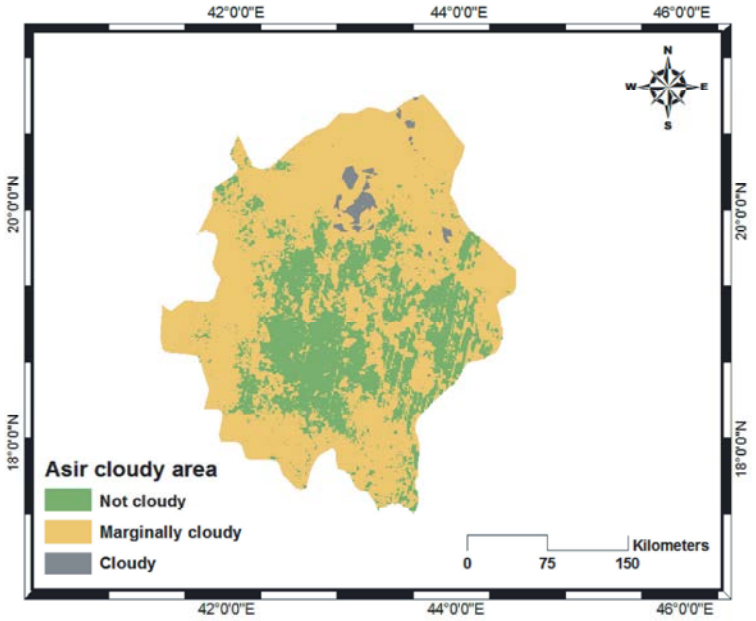

Fig. 9: Spatiotemporal distribution of the total cloud probability map of Asir region in KSA from January 2006 to October 2011

and cloudy area is about: 1145 km^2 (1.5%) of the total area Asir region (77088 km^2).

It is not easy to compare different algorithm of cloud detection because the different setting and requirements of each technique. The current algorithm proved to be efficient in cloud detection over agricultural land and desert [22, 23, 28].

Using different flags for cloud detection methodology produced qualitative and reliable results in corresponding to the infrared window channel exits in MERIS data. Frey *et al*. [26] reported that different flags indicated that different cloud flags can do quite well in capturing the gross cloud features on this day and time. Flags capture the obvious cold clouds observed in the infrared image, but some differences exist in cloud detection for low (warm) clouds over the ocean and land regions.

According to McNally and Watts [29], an interesting feature in the Mediterranean image is a swath of what is believed to be aerosol. The scheme has obviously reacted to the adopted methodology and flagged the area cloudy in correlation to the sensitivity to Saharan dust [30].

CONCLUSIONS AND RECOMMENDATIONS

The aim of the present work is to apply the cloud probability algorithm developed by the Institute for Space Science, Free University Berlin. The implementation of the algorithm resulted in a robust cloud probability maps over the designated area. The classification of the resulted maps into two classes cloudy and not cloudy eases the sum of all the cloudy pixels of the 59 probability maps conducted. The spatiotemporal distribution of the clouds raises the quest for the proper use of such a methodology. The correlation between the cloudy pixels and land use land cover beneath is the keystone of proper practice of the current approach. As the clouds are the main source of precipitation so the utilization of the cloud probability maps will be strongly correlated to water resources management in the area. The practices of water resources management are numerous but the present methodology helps decision makers to decide where the dams need to be built in order to increase the potentials of ground water recharge as a direct implementation of the adopted methodology. Moreover, several applications of integrated water resources management or risk assessments may benefits from the current methodology, i.e.: estimation of soil moisture content, improvement of rainfed agriculture and/or to produce risk maps to avoid the drastic consequences of flooding events that may occur. Further work regarding the correlation between the cloud probability maps and land use land cover beneath may need to be carried out.

REFERENCES

1. Winston, J.S., 1976. Planetary-scale characteristics of monthly mean longwave radiation and albedo and some year-to-year variations, Mon. Weather Review, 95: 235-256.
2. Stephens, G.L., G.G. Campbell and T.H. Vonder Haar, 19981. Earth radiation budgets, Journal of Geophysics Research, 86: 9739-9760.
3. Simpson, J., 1999. Improved cloud detection and cross-calibration of ATSR, MODIS and MERIS data. In (ESA-SP-479), E.P.D., editor, ATSR International Workshop on the Applications of the ERS along track scanning radiometer.
4. Goodman, A.H. and A. Henderson-Sellers, 1988. Cloud detection analysis: A review of recent progress. Atmospheric Research, 21: 203-221.
5. Rossow, W.B., 1989. Measuring cloud properties from space: A review. Journal of Climate, 2: 201-213.
6. Rossow, W.B., F. Mosher, E. Kinsella, A. Arking, M. Desbois, E. Harrison, P. Minnis, E. Ruprecht, G. Seze, C. Simmer and E. Smit, 1985. ISCCP cloud algorithm intercomparison. Journal of Climate and Applied Meteorology, 24: 877-892.
7. Coakley, J.A. and F.P. Bretherton, 1982. Cloud cover from high-resolution scanner data: Detecting and allowing for partially filled fields of view. Journal of Geophysics Research, 87: 4917-4936.
8. Tovinkere, V.R., M. Penaloza, A. Logar, J. Lee, R.C. Weger, T.A. Berendes and R.M. Welch, 1993. An intercomparison of artificial intelligence approaches for polar scene identification. Journal of Geophysics Research, 98: 5001-5029.
9. Ebert, E.E., 1987. A pattern recognition technique for distinguishing surface and cloud types in the Polar Regions. Journal of Climate and Applied Meteorology, 26: 1412-1431.
10. Gallaudet, T.C. and J.J. Simpson, 1991. Automated cloud screening of AVHRR imagery using split-and-merge clustering. Remote Sensing of Environment, 38: 77-100.
11. Delwart, S., R. Preusker, L. Bourg, R. Santer, D. Ramon and J. Fischer, 2007. MERIS inflight spectral calibration. International Journal of Remote Sensing, 28: 479-496.
12. Brockmann, C., A. Ruescas and K. Stelzer, 2011. MERIS pixel identification. ATBD, 2-17, ESA-ESRIN.
13. Fischer, J. and H. Grassl, 1991. Detection of cloud-top height from backscattered radiances within the oxygen A band. Part 1: Theoretical study. Journal of Applied Meteorology, 30: 1245-1259.
14. Fell, F. and J. Fischer, 2001. Numerical simulation of the light field in the atmosphere-ocean system using the matrix-operator method. Journal of Quantitative Spectroscopy and Radiative Transfer, 3: 351-388.
15. Lindstrot, R., R. Preusker and J. Fischer, 2009. The retrieval of land surface pressure from MERIS measurements in the Oxygen A band. American Meteorological Society, pp: 1367-1377.
16. King, M.D., Y.J. Kaufman, W.P. Menzel and D. Tanré, 1992. Remote sensing of cloud, aerosol and water vapor properties from the Moderate Resolution Imaging Spectrometer (MODIS). IEEE Transactions on Geoscience and Remote Sensing, 30: 1-27.
17. Saunders, R.W. and R.T. Kriebel, 1988. An improved method for detecting clear sky and cloudy radiances from AVHRR data. International Journal of Remote Sensing, 9: 123-150.
18. McClatchey, R., R. Fenn, J. Selby, F. Volz and J. Garing, 1972. Optical properties of the atmosphere. 3rd ed. AFCRL-72- 0497, Environmental Research Paper 411, pp: 108.
19. ESRI, 2008. ArcMap. Version 9.3 User manual. Redlands, CA, USA, pp: 135-137.
20. Petty, G.W., 2006. A first course in atmospheric radiation. Sundog Publishing, pp: 460.
21. Hawkinson, J.A., W. Feltz, T.J. Schmit, A.J. Schreiner and S.A. Acherman, 2001. A validation study of the GOES sounder cloud top pressure product, 11th Conference on Satellite Meteorology and Oceanography. American Meteorological Society, pp: 348-350.
22. Fischer, J. and R. Bennartz, 1997. Retrieval of total water vapour content from MERIS measurements, Algorithm Theoretical Basis Document PO-TN-MEL-GS-0005, ESA-ESTEC, Noordwijk, Netherlands.
23. Lindstrot, R., R. Preusker and J. Fischer, 2010. The empirical correction of stray light in theMERIS oxygen A band channel, Journal of Atmosphere and Oceanic Technology, 27(7): 1185-1194.
24. Elhag, M., A. Psilovikos, I. Manakos and K. Perakis, 2011. Application of the SEBS water balance model in estimating daily evapotranspiration and evaporative fraction from remote sensing data over the Nile Delta. Water Recourses Management, 25: 2731-2742.

25. Guan, N.H., M. Zubir, M. Jafri and K. Abdullah, 2010. Improved cloud detection technique at South China sea. Aerospace Technologies Advancements, SBN 978-953-7619-96-1, pp: 492.
26. Frey, R.A., S.A. Ackerman, Y. Liu, K.I. Strabala, H. Zhang, J.R. Key and X. Wang, 2008. Cloud detection with MODIS. Part I. Improvemetns in the MODIS cloud mask for collection 5. Journal of Technology, 25: 1057-1072.
27. Jedlovec, G.J., S.L. Haines and F.J. LaFontaine, 2008. Spatial and temporal varying thresholds for cloud detection in GOES imagery. IEEE Trans. Geoscience of Remote Sensing, 46(6): 1705-1717.
28. Fischer, J., R. Preusker and L. Schüller, 1997. ATBD cloud top pressure. European Space Agency Algorithm Theoretical Basis Doc. PO-TN-MEL-GS-0006, pp: 28.
29. McNally, A.P. and P.D. Watts, 2003. A cloud detection algorithm for high spectral resolution in frared sounders. Quarterly Journal of the Royal Meteorological Society, 129: 3411-3423.
30. Weaver, C., P. Ginoux, C. Hsu, M. Chou and J. Joiner, 2001. Radiative forcing of Saharan dust. GOCART model simulations compared with ERBE data. Journal of the Atmospheric Sciences, 59(3): 736-747.